ENERGETICS OF FINE DOMAIN STRUCTURES

ANTONIO DESIMONE

Max-Planck Institute for Mathematics in the Sciences
Inselstr. 22-26, 04103 Leipzig
GERMANY

desimone@mis.mpg.de

Paper presented at the 5th International Symposium on
Ferroic Domains and Mesoscopic Structures,
ISFD-5, Penn State University, 6-10 April 1998.

Published in: *Ferroelectrics*, 1999, Vol. 222, pp. 275-284.

Ferroelectrics, 1999, Vol. 222, pp. 275-284.

ENERGETICS OF FINE DOMAIN STRUCTURES

ANTONIO DESIMONE
Dipartimento di Ingegneria Civile, Università di Roma "Tor Vergata",
00133 Roma, Italy

In the last few decades, new mathematical tools have become available for the analysis of minimization problems involving non-convex free-energies. These advances have shed some new light on the behavior of a variety of physical systems exhibiting domain structures, and on their response to external actions (forces, electromagnetic fields, etc.). Examples range from ferroelastic solids (in particular, shape memory alloys) to ferromagnetic and ferroelectric materials (in particular, solids with strong electro- or magneto-elastic coupling). In this paper, striped domain patterns observed in liquid crystalline polymers are discussed, showing that the emergence of domain structures, and the success of the mathematical techniques for their analysis are not peculiar to crystalline solids.

Keywords: elastomers; liquid crystals; calculus of variations; convexity.

GENERAL PRINCIPLES

It is widely acknowledged that the emergence of equilibrium domain structures can be often given an energetic interpretation. In fact, for a system described by a non-convex free-energy density (a **multiwell potential**) like the one schematically described in Figure 1, configurations such that the state variables take only values for which the free-energy is minimal (i.e., the state variables lie in the material's **energy wells**) are energetically appealing.

Whenever external causes do not allow the system to rest entirely on only one such well (**frustration of the spatially uniform states**), domain structures are to be expected. These may evolve through the application of external 'loads' (**domain switching**) and their typical size is often established through the competition of bulk energies, including the aforementioned multiwell potential, which promote domain refinement, and some form of interfacial energy which penalizes the spatial oscillations of the state variables (**scale selection**).

Armed with this simple, yet very powerful unifying conceptual scheme, one can go a long way in the qualitative understanding of domain structures in a wide variety of physical systems. The identification of the relevant state variables is always the first step in such an endeavour. The example chosen in this paper has the aim of illustrating some of the subtleties that need to be confronted when the state variables have a more complicated structure that the one tacitly implied by the graph of Figure 1, where a scalar state variable is envisioned.

NEMATIC ELASTOMERS: STRUCTURE OF THE ENERGY WELLS

Nematic elastomers are anisotropic rubbers for which the state variables can be sometimes reduced to a tensor-valued field $\mathbf{F}$, the deformation gradient, and a vector field $\mathbf{n}$, the director. The deformation gradient must satisfy a kinematic compatibility condition: It must be the gradient of a continuous function $\mathbf{y}$ which maps the reference configuration Ω into the deformed configurations $\mathbf{y}(\Omega)$. Thus,

$$\mathbf{F}(\mathbf{x}) = \nabla \mathbf{y}(\mathbf{x})\,, \quad \mathbf{x} \in \Omega\,, \tag{1}$$

for some continuous $\mathbf{y}$. Typically one accepts that rubbers are essentially incompressible, so that one also has

$$\det \mathbf{F}(\mathbf{x}) = 1\,, \quad \mathbf{x} \in \Omega\,. \tag{2}$$

The director field $\mathbf{n}$ is a unit vector field,

$$|\mathbf{n}(\mathbf{x})| = 1\,, \quad \mathbf{x} \in \Omega\,, \tag{3}$$

describing at each point of the body the average orientation of the nematic elements of the molecules making up the elastomer. Under the assumption that the molecular network of the rubber can be described through anisotropic gaussian chains, Warner and Terentjev[1] have derived an expression for the free-energy of a nematic elastomer which can be reduced to

$$\varphi(\mathbf{F},\mathbf{n}) = \frac{\mu}{2}\left(r^{\frac{1}{3}}\left[\mathrm{tr}\,(\mathbf{F}\mathbf{F}^T) - \frac{r-1}{r}(\mathbf{F}\mathbf{F}^T)\mathbf{n}\cdot\mathbf{n}\right] - 3\right) . \tag{4}$$

Here $\mathbf{F}^T$ denotes the transpose of $\mathbf{F}$, tr stands for trace, while $\mu > 0$ and $r > 1$ are two material constants, respectively, the rubber energy scale (i.e., the shear modulus corresponding to $r = 1$) and the backbone anisotropy (i.e., the mean ratio of chain dimensions in the directions parallel and perpendicular to the director). Note that for $r = 1$, the value of the backbone anisotropy parameter above the nematic transition temperature, (4) becomes the standard (neo-hookean) isotropic free-energy density, a function of the deformation gradient only, which is minimized at $\mathbf{F} = \mathbf{I}$, the identity tensor. However, when $r > 1$, an easy calculation shows that

$$\min_{\det\mathbf{F}=1\,,|\mathbf{n}|=1} \varphi = \frac{\mu}{2}\left(r^{\frac{1}{3}}\left[\frac{1}{r}\lambda_1 + \lambda_2 + \lambda_3\right] - 3\right) = 0\,, \tag{5}$$

where $\lambda_1 \geq \lambda_2 \geq \lambda_3$ are the eigenvalues of $\mathbf{F}\mathbf{F}^T$, and that this minimum value of the energy is attained by any pair $(\mathbf{F},\mathbf{n})$ such that $\frac{1}{r}\lambda_1 = \lambda_2 = \lambda_3 = r^{-\frac{1}{3}}$ and $\mathbf{n}$ is the eigenvector of $\mathbf{F}\mathbf{F}^T$ corresponding to the largest eigenvalue λ_1. Equivalently, every pair $(\mathbf{U}_\mathbf{n},\mathbf{n})$, where $\mathbf{n}$ is a unit vector and

$$\mathbf{U}_\mathbf{n} = r^{\frac{1}{3}}\mathbf{n}\otimes\mathbf{n} + r^{-\frac{1}{6}}\left(\mathbf{I} - \mathbf{n}\otimes\mathbf{n}\right)\,, \tag{6}$$

(here $\otimes$ denotes the tensor product of two vectors) is a minimizer of φ. Note that the deformation described by $\mathbf{U}_\mathbf{n}$ is the one that maps a ball of radius one onto a prolate spheroid of major axis $r^{\frac{1}{3}}$ parallel to $\mathbf{n}$. Since, by frame indifference, $\varphi(\mathbf{R}\mathbf{F},\mathbf{R}\mathbf{n}) = \varphi(\mathbf{F},\mathbf{n})$ for every rotation $\mathbf{R}$, the energy wells of the material at hand can be described mathematically by the formula

$$\mathbb{K} = \mathbb{K}_{el}\times S^2 = \bigcup_{\mathbf{n}\in S^2} \mathrm{SO}(3)(\mathbf{U}_\mathbf{n},\mathbf{n})\,, \tag{7}$$

where S^2 is the sphere of radius one describing the unit vectors of $\mathbb{R}^3$, while SO(3) is the group of rotations in $\mathbb{R}^3$. Figure 2 gives a schematic description of the set $\mathbb{K}$.

NEMATIC ELASTOMERS: SOFT DEFORMATIONS

Consider a sheet parallel to the yz plane which is initially in the zero energy configuration described by $\mathbf{F}_0 = \mathbf{U}_{\mathbf{e}_3}$, $\mathbf{n}_0 = \mathbf{e}_3$ (here $\mathbf{e}_1$, $\mathbf{e}_2$, $\mathbf{e}_3$, are the three orthonormal vectors parallel to the xyz axes of a given right-handed cartesian frame), and assume that the specimen is stretched along the y axis, so that the macroscopic deformation of the sheet is

$$\mathbf{F}_t = \begin{bmatrix} r^{-\frac{1}{6}} & 0 & 0 \\ 0 & \lambda(t) & 0 \\ 0 & 0 & \frac{r^{\frac{1}{6}}}{\lambda(t)} \end{bmatrix}, \quad r^{-\frac{1}{6}} = \lambda(0) \leq \lambda(t) \leq \lambda(1) = r^{\frac{1}{3}}, \tag{8}$$

with $\lambda(t)$ an increasing function of $t \in [0,1]$. Clearly, with the definition above, $\mathbf{F}_1 = \mathbf{U}_{\mathbf{e}_2}$. Since for $t \neq 0,1$ the eigenvalues of $\mathbf{F}_t\mathbf{F}_t^T$ do not satisfy the condition $\frac{1}{r}\lambda_1 = \lambda_2 = \lambda_3$, the uniform deformation with gradient $\mathbf{F}_t$ has positive energy. However, for $\delta^2(t) = \frac{1}{\lambda(t)}(\lambda^2(t) - r^{-\frac{1}{3}})(r^{\frac{2}{3}} - \lambda^2(t))$, the tensors

$$\mathbf{F}_t^{\pm} = \begin{bmatrix} r^{-\frac{1}{6}} & 0 & 0 \\ 0 & \lambda(t) & \pm\delta(t) \\ 0 & 0 & \frac{r^{\frac{1}{6}}}{\lambda(t)} \end{bmatrix}, \quad \mathbf{F}_t^{+} - \mathbf{F}_t^{-} = 2\delta(t)\mathbf{e}_2 \otimes \mathbf{e}_3 \tag{9}$$

satisfy the eigenvalue conditions guaranteeing that $\mathbf{F}_t^{\pm} \in \mathbb{K}_{el}$. Therefore, if $\mathbf{n}_t^{\pm}$ is the eigenvector corresponding to the maximum eigenvalue of $(\mathbf{F}_t^{\pm})(\mathbf{F}_t^{\pm})^T$, the pairs $(\mathbf{F}_t^{+}, \mathbf{n}_t^{+})$, $(\mathbf{F}_t^{-}, \mathbf{n}_t^{-})$ lie on the energy wells. In addition, as shown by the second formula in (9), they differ by the rank-one tensor $2\delta(t)\mathbf{e}_2 \otimes \mathbf{e}_3$. It follows that we can in fact construct a continuous deformation whose gradient takes the values $\mathbf{F}_t^{+}$, $\mathbf{F}_t^{-}$ on stripes orthogonal to $\mathbf{e}_3$. Indeed, for k integer, and denoting by χ the one-periodic function taking the value zero in $[0, \frac{1}{2})$ and the value one in $[\frac{1}{2}, 1)$, the deformation

$$\mathbf{y}^k(\mathbf{x}) = \mathbf{F}_t^{-}\mathbf{x} + \frac{2\delta(t)}{k}\mathbf{e}_2 \int_0^{k\mathbf{x}\cdot\mathbf{e}_3} \chi(\mathrm{s})\,\mathrm{ds} \tag{10}$$

has the required properties. Note that $\frac{1}{k}$ is proportional to the width of the stripes and, as $k \to \infty$, $\mathbf{y}^k$ converges uniformly to the affine deformation

$$\mathbf{y}(\mathbf{x}) = \left(\frac{1}{2}\mathbf{F}_t^{-} + \frac{1}{2}\mathbf{F}_t^{+}\right)\mathbf{x} = \mathbf{F}_t\mathbf{x}, \tag{11}$$

where the factors $\frac{1}{2}$ arise from the fact that $\mathbf{F}_t^{+}$ and $\mathbf{F}_t^{-}$ occupy the same volume fraction (namely, $\frac{1}{2}$) of the specimen.

The discussion above summarizes Warner and Terentjev's[1] interpretation of the experimental observation of striped domain patterns by Kundler and Finkelmann[2]. In fact, let

$$\Phi(\mathbf{F}) = \min_{|\mathbf{n}|=1} \varphi(\mathbf{F}, \mathbf{n}). \tag{12}$$

Then, since Φ is not convex along the rank-one line that joins $\mathbf{F}_t^+$ and $\mathbf{F}_t^-$ in matrix space:

$$(13) \qquad \Phi\left(\mathbf{F}_t^- + \frac{1}{2}(\mathbf{F}_t^+ - \mathbf{F}_t^-)\right) > \Phi(\mathbf{F}_t^-) + \frac{1}{2}\left(\Phi(\mathbf{F}_t^+) - \Phi(\mathbf{F}_t^-)\right) = 0\,,$$

$$(14) \qquad \mathbf{F}_t = \mathbf{F}_t^- + \frac{1}{2}(\mathbf{F}_t^+ - \mathbf{F}_t^-)\,,$$

it is always energetically advantageous to replace the uniform macroscopic deformation $\mathbf{F}_t$ with a nonuniform (mesoscopic) domain pattern with macroscopic average $\mathbf{F}_t$, but such that the deformation gradients are locally $\mathbf{F}_t^-$ and $\mathbf{F}_t^+$. As $\lambda(t)$ is increased from $r^{-\frac{1}{6}}$ to $r^{\frac{1}{3}}$, the sheet may follow a zero-energy path (hence a path along which the system could, in principle, evolve without developing internal stresses) joining the states $(\mathbf{U}_{\mathbf{e}_3}, \mathbf{e}_3)$ and $(\mathbf{U}_{\mathbf{e}_2}, \mathbf{e}_2)$, resulting in the macroscopic stretch $r^{\frac{1}{3}}/r^{-\frac{1}{6}} = \sqrt{r}$ along the y axis (cf. Figure 3).

It should be noted, however, that the one described above is not the only soft path joining the uniform states $(\mathbf{U}_{\mathbf{e}_3}, \mathbf{e}_3)$ and $(\mathbf{U}_{\mathbf{e}_2}, \mathbf{e}_2)$. An alternative one (indeed, one of the many that are possible) is shown in Figure 4, and it is obtained with a more complicated construction (a laminate of laminates), in which the deformation gradients take values only (with the exception of transition layers of negligible size and energetic content) on the two wells $(\mathrm{SO}(3)\mathbf{U}_{\mathbf{e}_3}, \mathrm{SO}(3)\mathbf{U}_{\mathbf{e}_2})$. Domain patterns of this type are often observed in crystalline solids undergoing martensitic phase transitions[3]. In this case $\mathbf{U}_{\mathbf{e}_3}$ and $\mathbf{U}_{\mathbf{e}_2}$ would represent two of a discrete number of martensitic energy wells, related to one another by crystallographic symmetry transformations. More precisely, $\mathbf{U}_{\mathbf{e}_3}$ and $\mathbf{U}_{\mathbf{e}_2}$ could be two of the three low symmetry, tetragonal, martensitic variants arising from a high symmetry, cubic, austenitic parent phase.

CONVEXITY OF THE FREE-ENERGY DENSITY

The energetic interpretation of the emergence of domain patterns discussed in the previous section is based on the fact that a system may find an energetic advantage in letting its state variables develop fine scale spatial oscillations, while their macroscopic averages are held fixed. One may ask oneself for conditions on the free-energy of the system which lead to, or forbid this kind of behavior. With reference to the case where the state variable is a deformation gradient, one may ask which convexity properties of the free-energy, say Ψ, guarantee that a uniform deformation is always the energy minimizer under its own boundary conditions:

$$\Psi(\mathbf{F}) \leq \frac{1}{\text{volume}(\Omega)} \int_{\Omega} \Psi\left(\mathbf{F} + \nabla\theta(\mathbf{x})\right) \mathrm{d}\mathbf{x}\,, \tag{15}$$

where $\theta(\mathbf{x})$ is an arbitrary (Lipschitz) perturbation of the affine deformation $\mathbf{Fx}$, which vanishes on the boundary of Ω. A function Ψ that satisfies the inequality above is called quasiconvex. This property is 'intermediate' between the weaker notion of rank-one convexity (the property of being convex along rank-one lines), and the stronger notion of polyconvexity (a polyconvex function of $\mathbf{F}$ is a convex function of the minors of $\mathbf{F}$). Convexity is even stronger, although all these notions collapse onto the same one when the state variable is a scalar or a vector. Although quasiconvexity is the property more closely linked to physical intuition, it is the hardest to check. On the contrary, it is relatively easy to check for rank-one convexity or polyconvexity, but there is a gap between these two notions, and quasiconvexity sits in the middle. Interestigly, with nematic elastomers we jump from one to the other side of this gap when crossing the nematic transition temperature. At low temperatures $r > 1$, and (13) shows that the free-energy fails to be rank-one convex: Indeed we can lower the system's energy by layering along rank-one lines. In the high temperature isotropic phase the free-energy is polyconvex, hence quasiconvex, and uniform deformations prevail.

The interested reader is referred to the bibliography[4],[5] for expositions of the recent mathematical developments on the minimization of non-convex free-energy functionals from which this paper draws freely, and for extensive lists of references.

THE PHYSICS IN THE DETAILS

Although a lot can be understood with unifying conceptual schemes, the peculiarities of a physical system are often hidden in the details. In the example of this paper, we went a long way by ignoring many geometric details, such as how close should the mesoscopic pattern be to its macroscopic average. We accomplished this by ignoring surface energy, hence losing information about the actual scale of the domains. By focussing on the asymptotic features of the patterns, but allowing the size of the domains to shrink to zero, we have produced a multiplicity of energetically (asymptotically) equivalent domain patterns, two of which are shown in Figures 3 and 4.

Finkelmann et al.[6] suggest that the scale of the striped domain patterns is established by the competition of surface energy at the domain interfaces (which favours domain coarsening) and the global geometric constraints imposed by the clamps on the rubber sheet (these promote refinement as a way of relaxing the stresses that would arise due to the mismatch between the available zero energy mesoscopic deformations and the uniform ones which are imposed macroscopically: Indeed, in our system, this is the frustrating 'agent' that prevents configurations from being both uniform and on the energy wells). In the pattern of Figure 4, extra elastic energy arises at the interfaces where the two finely layered structures meet, unless the fineness of the pattern is infinite. Maybe this is enough to select the pattern of Figure 3 as the preferred one. Even so, the general question of how to select, among the many available low-energy paths, the ones that are indeed dynamically accessible for a given loading history, arises. In addition, an even more important issue is that in the 'real' elastomeric system, low-energy deformation paths are not really soft but only semi-soft: some stress is actually needed to stretch the rubber sheet. Finkelmann et al.[6] do succeed in incorporating the effect in their model, at least for the easy deformation path of Figure 3. How to correct for 'semi-softness' along more general deformation paths, or in other physical systems exhibiting similar behavior? Progress on these issues will be hard, but rewarding, as some recent papers[7] may induce us to believe.

Acknowledgments
The author thanks G. Dolzmann, S. Müller, and E.M. Terentjev for their readiness in discussing, orally or in writing, issues related to the subject matter of this paper.

References

[1.] M. Warner and E.M. Terentjev, *Prog. Polym. Sci.*, **21**, 853 (1996).
[2.] I. Kundler and H. Finkelmann, *Makromol. Chem. Rapid Commun.*, **16**, 679 (1995).
[3.] J.M. Ball and R.D. James, *Phil Trans. Roy. Soc. Lon. A*, **338**, 389 (1992).
[4.] B. Dacorogna, *Direct Methods in the Calculus of Variations*, Springer-Verlag, New York, 1989.
[5.] S. Müller, *Variational Models for Microstructures and Phase Transitions*, Springer Lecture Notes in Mathematics, forthcoming.
[6.] H. Finkelmann, I. Kundler, E.M. Terentjev, and M. Warner, *J. Phys. II France*, **7**, 1059 (1997).
[7.] R.V. Kohn and F. Otto, *Physica D*, **107**, 272 (1997).

FIGURE 2. A sketch of the energy wells for nematic elastomers (backbone anisotropy parameter $r > 1$). $\mathbf{R}$ and $\mathbf{Q}$ are arbitrary rotations.

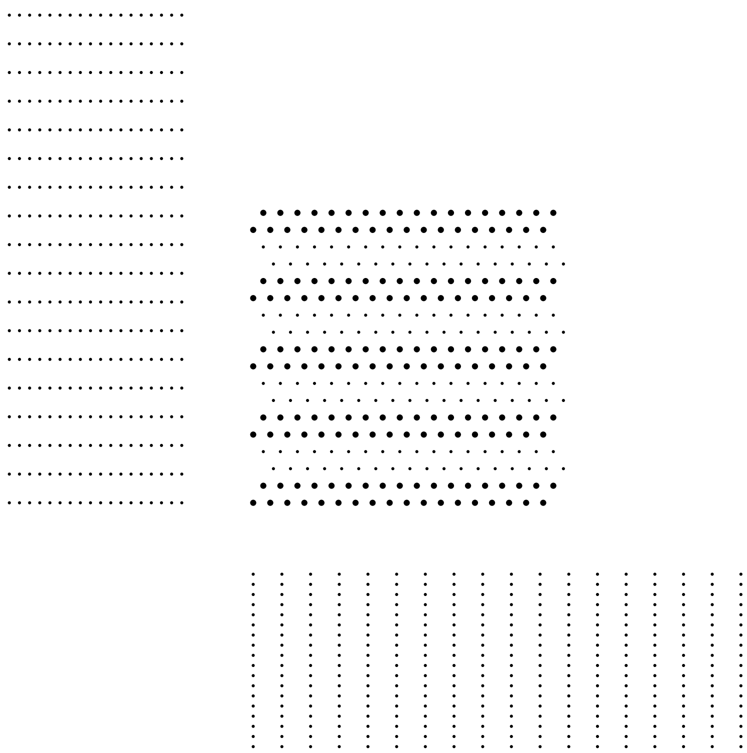

FIGURE 3. The soft deformation path from $\mathbf{U}_{\mathbf{e}_3}$ (top left) to $\mathbf{U}_{\mathbf{e}_2}$ (bottom right) of Warner and Terentjev. Here, as in the picture below, the shading hints at the different optical contrast induced in polarized light by the director.

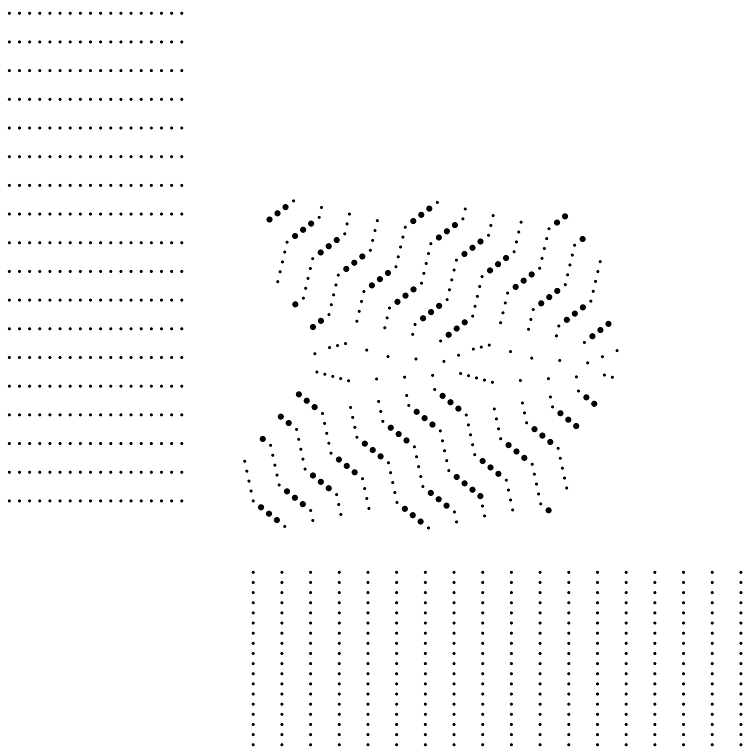

FIGURE 4. An alternative soft deformation path from $\mathbf{U}_{\mathbf{e}_3}$ (top left) to $\mathbf{U}_{\mathbf{e}_2}$ (bottom right).